World Journal of Gastroenterology

Submit a Manuscript: http://www.wjgnet.com/esps/
Help Desk: http://www.wjgnet.com/esps/helpdesk.aspx
DOI: 10.3748/wjg.v22.i13.3652

World J Gastroenterol 2016 April 7; 22(13): 3652-3662
ISSN 1007-9327 (print) ISSN 2219-2840 (online)

ORIGINAL ARTICLE

Observational Study

Dual-input two-compartment pharmacokinetic model of dynamic contrast-enhanced magnetic resonance imaging in hepatocellular carcinoma

Jian-Feng Yang, Zhen-Hua Zhao, Yu Zhang, Li Zhao, Li-Ming Yang, Min-Ming Zhang, Bo-Yin Wang, Ting Wang, Bao-Chun Lu

Jian-Feng Yang, Min-Ming Zhang, Department of Radiology, Second Affiliated Hospital, College of Medicine, Zhejiang University, Hangzhou 310009, Zhejiang Province, China

Jian-Feng Yang, Shaoxing People's Hospital (Shaoxing Hospital of Zhejiang University), Shaoxing 312000, Zhejiang Province, China

Zhen-Hua Zhao, Yu Zhang, Li Zhao, Li-Ming Yang, Bo-Yin Wang, Ting Wang, Department of Radiology, Shaoxing People's Hospital (Shaoxing Hospital of Zhejiang University), Shaoxing 312000, Zhejiang Province, China

Bao-Chun Lu, Department of Hepatobiliary Surgery, Shaoxing People's Hospital (Shaoxing Hospital of Zhejiang University), Shaoxing 312000, Zhejiang Province, China

Author contributions: Yang JF and Zhao ZH contributed equally to this work; Yang JF, Zhao ZH and Zhang MM designed the research; Zhang Y, Zhao L, Yang LM, Wang BY, Wang T and Lu BC performed the research; Zhang Y and Zhao L analyzed the data; and Yang JF wrote the paper.

Supported by Public Welfare Projects of Science Technology Department of Zhejiang Province, No. 2014C33151; Medical Research Programs of Zhejiang province, No. 2014KYA215, No. 2015KYB398, No. 2015RCA024 and No. 2015KYB403; and Research Projects of Public Technology Application of Science and Technology of Shaoxing City, No. 2013D10039.

Institutional review board statement: The study was reviewed and approved by the Ethics Committee of Shaoxing People's Hospital (Shaoxing Hospital of Zhejiang University).

Informed consent statement: All study participants, or their legal guardian, provided informed written consent prior to study enrollment.

Conflict-of-interest statement: The authors declare that there is no conflict of interest.

Data sharing statement: No additional data are available.

Correspondence to: Min-Ming Zhang, Professor, Chief, Department of Radiology, Second Affiliated Hospital, College of Medicine, Zhejiang University, 88 Jiefang Road, Hangzhou 310009, Zhejiang Province, China. zhangminming@zju.edu.cn
Telephone: +86-571-87315255
Fax: +86-571-87315255

Received: October 26, 2015
Peer-review started: October 27, 2015
First decision: December 11, 2015
Revised: December 15, 2015
Accepted: December 30, 2015
Article in press: December 30, 2015
Published online: April 7, 2016

Abstract

AIM: To investigate the feasibility of a dual-input two-compartment tracer kinetic model for evaluating tumorous microvascular properties in advanced hepatocellular carcinoma (HCC).

METHODS: From January 2014 to April 2015, we prospectively measured and analyzed pharmacokinetic parameters [transfer constant (K_{trans}), plasma flow

(F_p), permeability surface area product (PS), efflux rate constant (k_{ep}), extravascular extracellular space volume ratio (v_e), blood plasma volume ratio (v_p), and hepatic perfusion index (HPI)] using dual-input two-compartment tracer kinetic models [a dual-input extended Tofts model and a dual-input 2-compartment exchange model (2CXM)] in 28 consecutive HCC patients. A well-known consensus that HCC is a hypervascular tumor supplied by the hepatic artery and the portal vein was used as a reference standard. A paired Student's *t*-test and a nonparametric paired Wilcoxon rank sum test were used to compare the equivalent pharmacokinetic parameters derived from the two models, and Pearson correlation analysis was also applied to observe the correlations among all equivalent parameters. The tumor size and pharmacokinetic parameters were tested by Pearson correlation analysis, while correlations among stage, tumor size and all pharmacokinetic parameters were assessed by Spearman correlation analysis.

RESULTS: The F_p value was greater than the PS value (F_p = 1.07 mL/mL per minute, PS = 0.19 mL/mL per minute) in the dual-input 2CXM; HPI was 0.66 and 0.63 in the dual-input extended Tofts model and the dual-input 2CXM, respectively. There were no significant differences in the k_{ep}, v_p, or HPI between the dual-input extended Tofts model and the dual-input 2CXM (P = 0.524, 0.569, and 0.622, respectively). All equivalent pharmacokinetic parameters, except for v_e, were correlated in the two dual-input two-compartment pharmacokinetic models; both F_p and PS in the dual-input 2CXM were correlated with K_{trans} derived from the dual-input extended Tofts model (P = 0.002, r = 0.566; P = 0.002, r = 0.570); k_{ep}, v_p, and HPI between the two kinetic models were positively correlated (P = 0.001, r = 0.594; P = 0.0001, r = 0.686; P = 0.04, r = 0.391, respectively). In the dual input extended Tofts model, v_e was significantly less than that in the dual input 2CXM (P = 0.004), and no significant correlation was seen between the two tracer kinetic models (P = 0.156, r = 0.276). Neither tumor size nor tumor stage was significantly correlated with any of the pharmacokinetic parameters obtained from the two models (P > 0.05).

CONCLUSION: A dual-input two-compartment pharmacokinetic model (a dual-input extended Tofts model and a dual-input 2CXM) can be used in assessing the microvascular physiopathological properties before the treatment of advanced HCC. The dual-input extended Tofts model may be more stable in measuring the v_e; however, the dual-input 2CXM may be more detailed and accurate in measuring microvascular permeability.

Key words: Hepatocellular carcinoma; Dynamic contrast-enhanced magnetic resonance imaging; Pharmacokinetics

Core tip: Dynamic contrast-enhanced magnetic resonance imaging provides a more comprehensive assessment of microvascular parameters in tumors; however, selection of a pharmacokinetic model that takes into account actual physiopathological status is an essential component of evaluating tumor microvascular permeability and perfusion. Here, we confirm that a dual-input two-compartment tracer kinetic model is suitable for evaluating microvascular properties in advanced hepatocellular carcinoma.

Yang JF, Zhao ZH, Zhang Y, Zhao L, Yang LM, Zhang MM, Wang BY, Wang T, Lu BC. Dual-input two-compartment pharmacokinetic model of dynamic contrast-enhanced magnetic resonance imaging in hepatocellular carcinoma. *World J Gastroenterol* 2016; 22(13): 3652-3662 Available from: URL: http://www.wjgnet.com/1007-9327/full/v22/i13/3652.htm DOI: http://dx.doi.org/10.3748/wjg.v22.i13.3652

INTRODUCTION

Hepatocellular carcinoma (HCC) is one of the most common primary malignant tumors and the second leading cause of cancer-related deaths worldwide[1]. Some patients present with advanced disease at the time of diagnosis and are treated with molecular-targeted treatment, transarterial chemoembolization (TACE), and radiofrequency ablation against HCC[2]. Assessing the therapeutic efficacy of these therapy modalities is closely related to the tumorous microvasculature properties that are linked to the angiogenic potential of the tumor[3]. A tracer kinetic model of T1-weighted dynamic contrast-enhanced magnetic resonance imaging (DCE-MRI) has significant potential to obtain information about the tumor microvascular properties by estimating the pharmacokinetic parameters of the microvascular perfusion and permeability[4]. Some studies have shown the value of assessing microvascular properties in monitoring the effects of interventional therapy or antiangiogenic drug treatment of HCC, as well as metastases in the liver, by using single-input single-compartment or two-compartment tracer kinetic models to evaluate tumor pharmacokinetic parameters[3,5-8].

According to the dynamic distribution of the contrast agent, a well-mixed space of contrast agent is defined as a compartment where the contrast agent concentration is spatially uniform[9,10]. The tracer compartment model is divided into a single-compartment model such as the Tofts model, which assumes that the contrast agent is confined to only one compartment (*i.e.*, vascular space), and two-compartment models such as the extended Tofts model and the exchange model, in which the contrast

agent transits vascular space to the interstitial space[9]. The tissue under investigation and its underlying microvascular physiology, as well as the temporal resolution and spatial resolution of scanning MRI, are important factors that led us to select a tracer kinetic model. The parenchyma in most tumors consists of two compartments [tumorous intravascular space and extravascular extracellular space (EES)]; thus, a two-compartmental kinetic model may provide a better reflection of the microcirculation of tumor[11]. Moreover, HCC is supplied by both the portal vein and the hepatic artery in different proportions at various stages[12]. Therefore, we hypothesized that a dual-input two-compartment model may accurately evaluate the pharmacokinetic parameters in advanced HCC.

To date, microvascular property assessment by dual-input two-compartment tracer kinetic model with commonly used extracellular gadoliniun contrast agent has not been reported in HCC in a clinical practice setting. Hence, the aim of this study was to prospectively explore whether a dual-input two-compartment tracer kinetic model could evaluate the tumorous microvascular properties in advanced HCC by analyzing perfusion and permeability parameters derived from a dual-input extended Tofts model and a dual-input 2CXM.

MATERIALS AND METHODS

Patient population

This study was approved by the local Institutional Review Board, and informed consent was obtained from all patients. From January 2014 to April 2015, 42 patients with HCC were recruited, all of whom did not receive any antineoplastic treatment before their MRI scan. The inclusion and exclusion criteria are listed in Table 1. We staged Barcelxona-Clínic Liver Cancer classification (BCLC) for all enrolled HCC patients according to the criteria of the 2012 European Association for the Study of the Liver (EASL)[13]. Because microvascular physiologic parameters in tumors are functional biomarkers that could not be measured from the pathological sample *in vitro*, we looked to a well-known consensus as a reference standard that HCC is a hypervascular tumor supplied by both the portal vein and the hepatic artery in different proportions.

MRI technique

An MRI scan of the whole liver was performed using a 12-channel phased array body coil on the 3.0-T MRI system (Magnetom Verio, Siemens, Erlangen, Germany) with Syngo 2009B software. The scan protocol consisted of transverse T2-weighted turbo spin-echo images (TR/TE, 1370/81; slice thickness, 6 mm; interslice gap, 1.2 mm; matrix size, 207 × 320; received bandwidth, 220 kHz) and diffusion weighted

Table 1 Inclusion and exclusion criteria of the enrolled patients

Eligibility criteria	Exclusion criteria
Histopathology confirmed	MRI examination contraindication
Non-invasive diagnosis criteria [(EASL) 2012][1]	Significant renal insufficiency
Cirrhotic patients	
Hypervascular in the arterial phase	
Washout in the portal venous or delayed phase	
Non-antineoplaston therapy	Severe motion artifacts on MRI images
The largest diameter of lesion ⩾ 2 cm	Hepatic vein/portal cancer embolus
Age of patients ⩾ 18 yr	Inferior vena cava embolus
	Inability of informed written consent

[1]European Association for the Study of the Liver suggested non-invasive diagnosis criteria on 4-phase multidetector CT scan[13]. EASL: European Association for the Study of the Liver; MRI: Magnetic resonance imaging.

echoplanar images (TR/TE, 7400/73; slice thickness, 6 mm; interslice gap, 1.2 mm; *b* value = 0 s/mm², 600 s/mm²; matrix, 99 × 146; received bandwidth, 1802 kHz). Multi-flip angle T1 Mapping and DCE T1-weighted three-dimensional volume interpolated excitation (VIBE) fat-suppression sequence with breath-free (TR/TE, 3.5/1.17 msec; slice thickness, 5 mm; interslice gap, 1 mm; matrix, 288 × 164; field of view, 350 × 284 mm; scan slices were 30 in unenhanced T1WI and enhanced TIWI; flip angle were 5°, 10°, 15° in unenhanced TIWI, flip angle was 10° in enhanced TIWI; temporal resolution, 6 s) were also obtained. DCE-MR imaging data were acquired after a 5-s delay subsequent to the injection of contrast medium through a 20-guage peripheral intravenous line in the medial cubital vein (0.1 mmol/kg body weight of Gadodiamide contrast medium; Omniscan, GE Medical Systems, Amersham, Ireland) at 3.5 mL/s, followed by a saline chase of 20 mL at a rate of 2 mL/s. DCE-MR imaging included 35 acquiring phases and lasted for 227.5 s.

Model design

In this study, a dual-input two-compartment tracer kinetic model was utilized to analyze the perfusion and permeability of tumorous vascularity in HCC. This type of model accounts for the hepatic artery and portal vein input to the HCC and assumes contrast agent in two compartments (tumorous intravascular space and EES). We applied the hepatic perfusion index (HPI) to observe the contribution of arterial flow to the tumor. The tissue that the blood vessels containing contrast agent supply can be measured by Vascular Input Function (VIF) in both the hepatic artery and the portal vein. The definitions of all symbols are listed in Table 2.

The tracer in intravascular space is able to diffuse to the EES through the capillary walls, and K^{trans} denotes

Table 2 Summary of parameter terms used in the dual-input extended Tofts model and 2-compartment exchange model

Symbol	Definition	Unit
$C_{tiss}(t)$	Concentration of tracer in the tissue	mmol/L
$CA(t)$	Concentration of tracer in whole blood in a major feeding artery	mmol/L
$C_v(t)$	Concentration of tracer in the portal vein	mmol/L
Fa	Arterial fraction of the tissue perfusion	%
HLV	Hematocrit in major (large) vessels	none
HPI	Hepatic perfusion index	none
F_p	Flow rate of the blood plasma through the intravascular plasma space	mL/mL per minute
v_p	Ratio of blood plasma volume to tissue volume	%
v_e	Ratio of EES volume to tissue volume	%
k_{ep}	Efflux rate constant	min^{-1}
K_{trans}	Transfer constant	min^{-1}
PS	Endothelial permeability surface area product	mL/mL per minute
⊗	Convolution operator	None

EES: Extravascular extracellular space.

the tracer transfer constant between blood and EES, which combined the plasma flow (F_p) and the capillary permeability-surface area product (PS). The efflux rate constant (k_{ep}) is the ratio of the transfer constant from EES to blood plasma. v_p and v_e are the volume fraction in the vascular space and EES, respectively[14].

An extended Tofts model evaluates K_{trans}, v_e, v_p, and k_{ep}[14]. This model assumes that a neglect of plasma mean transit time results in a situation where the concentration of contrast agent within the plasma compartment is equal to the concentration in the supplying artery[15]; therefore, the concentration of contrast agent in the tissue, $C_{tiss}(t)$ in this model, can be written as follows:

$$C_{tiss}(t) = v_pCA(t)/(1\text{-}HLV) + K_{trans}CA(t)/(1\text{-}HLV)\otimes \exp(-k_{ep}t) \quad \text{(Eq. 1A)}$$

The equation (Eq. 1A) is the formulation of a single-input extended Tofts model; thus, we insert a dual inlet equation (Eq. 2) to produce the equation of the dual-input extended Tofts model (Eq. 1B).

$$CA(t)\rightarrow faCA(t) + (1\text{-}fa)C_v(t) \quad \text{(Eq. 2)}$$

$$C_{tiss}(t) = v_p[faCA(t) + (1\text{-}fa)C_v(t)]/(1 - HLV) + K_{trans}[faCA(t) + (1\text{-}fa)C_v(t)]/(1 - HLV)\otimes\exp(-k_{ep}t) \quad \text{(Eq. 1B)}$$

The 2CXM is the most common exchange model and can separately evaluate F_p and PS, in addition to V_p, V_e, and K_{ep}[10,14]. As for a single-input 2CXM, the concentration of the contrast agent in the tissue, Ctiss(t), can be written as follows:

$$C_{tiss}(t) = F_pCA(t)/(1 - HLV)\otimes A.\exp(-\alpha t) + (1\text{-}A).\exp(-\beta t) \quad \text{(Eq. 3A)}$$

We also insert a dual-inlet equation (Eq. 2) into the equation (Eq. 3A) to obtain the final equation of the dual-input 2CXM as follows:

$$C_{tiss}(t) = F_p[faCA(t) + (1 - fa)C_v(t)]/(1 - HLV\otimes A.\exp(-\alpha t) + (1 - A).\exp(-\beta t) \quad \text{(Eq. 3B)}$$

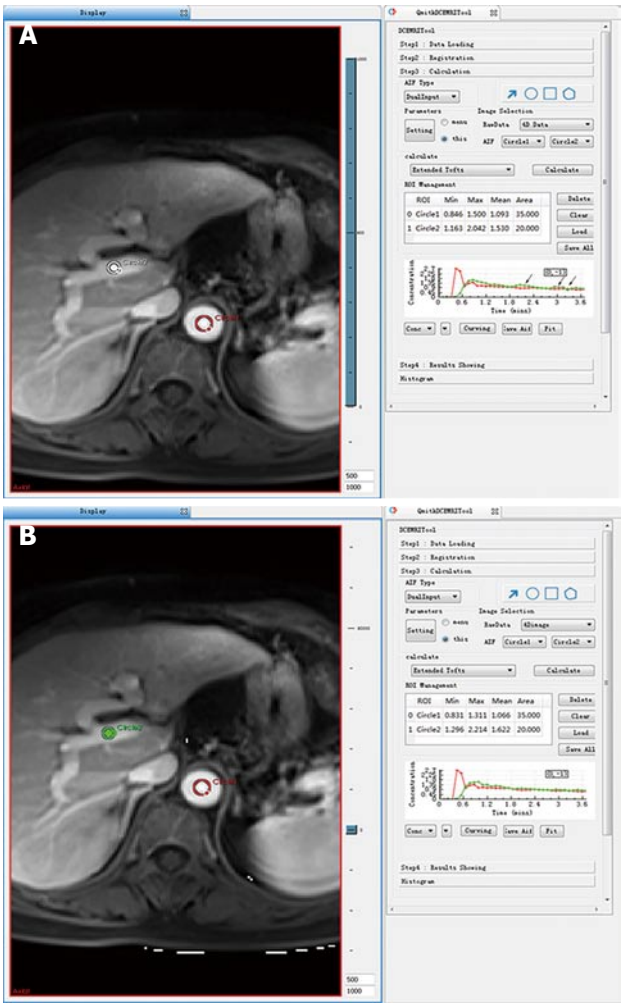

Figure 1 Concentration-time curve of the portal vein was an inferior fit (arrow) compared to that of the abdominal aorta without non-rigid registration (A); however, the concentration-time curve of the portal vein was a better fit after non-rigid registration (B).

where A, α, and β can be obtained from the model parameters v_p, v_e, and PS, respectively:

$A = PS/v_p$; $\alpha = PS/v_e$; $\beta = F_p/v_p$

Data postprocessing and analysis

Because there were more than 2 lesions of HCC in the liver in some patients, we measured the one with the largest diameter and also measured the mass volume. Each data set was measured by the same radiologist (who has 17 years of abdominal diagnosis experience), who kept the approach consistent at each time point of the procedure. All data were postprocessed using Omni Kinetics software (GE Healthcare, China). After data loading, we registered all acquired data using 3D non-rigid registration to relieve the motion artifact caused by breath and heart beating (Figure 1); then, we extracted an average signal-time course of the tumor and converted the signal-time curve to a concentration-time curve. The signal intensity of all pixels in the image was converted to contrast agent concentration using the precontrast T1 value of 1600

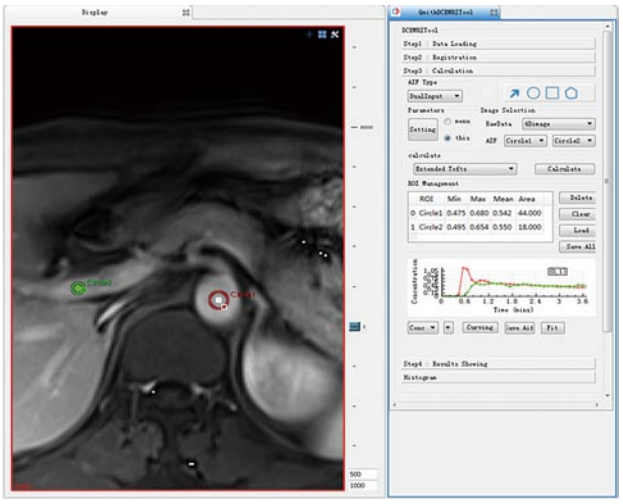

Figure 2 ROI 1 was placed on the abdominal aorta near the entrance of the celiac trunk, replacing the hepatic artery, and ROI 2 was placed on the portal vein as a dual input model to fit the vascular input function; the concentration-time curve maps of the ROI 1 and ROI 2 are shown to the right.

ms for blood and 1580 ms for tissue, and an assumed hematocrit of 0.42 was used to convert from whole blood concentration to plasma concentration for all patients. Before calculating the pharmacokinetic parameters, we drew the ROI on both the portal vein and the hepatic artery, which was replaced by the abdominal aorta near the entrance of celiac trunk as a dual-input model to fit the VIF (Figure 2). The size and location of the ROI drawn on the lesion in the same patient are consentaneous in both models. We drew the ROI (by hand) on the parenchyma of the HCC at its largest diameter on the T1WI images in each patient, avoiding necrosis, hemorrhage, steatosis, and peripheral blood vessels, and then, we used the dual-input extended Tofts model and the dual-input 2CXM, respectively, to fit the data and calculate tumorous perfusion and permeability parameters: K^{trans} in the dual-input extended Tofts model, F_P and PS in the dual-input 2CXM, and v_p, v_e, k_{ep}, and HPI in both models (Figure 3). All measurements were performed three times, and the mean value is presented.

Statistical analysis

Statistical analyses were performed with the SPSS statistical software package (version 19.0; SPSS Inc, Chicago, IL, United States). Tumor size and pharmacokinetic parameters were assessed by Pearson correlation analysis. Correlation between stage, tumor size and all pharmacokinetic parameters was assessed by Spearman correlation analysis. We compared all equivalent parameters obtained from the dual-input extended Tofts model and dual-input 2CXM using a paired Student's *t*-test or a nonparametric paired Wilcoxon rank sum test for non-normal distribution data to confirm the consistency of these two models. Pearson correlation analysis was also performed to analyze the correlation between all parameters. A *P*-value < 0.05 was considered statistically significant.

The statistical methods of this study were reviewed by Hai-yang Xing from Shaoxing University.

RESULTS

In this prospective study, 42 HCC patients based on pathological diagnosis and non-invasive criteria underwent T1WI DCE-MRI. However, 14 patients were excluded because of portal or hepatic vein/inferior vena cava embolus (6 patients), severe motion artifacts (4 patients), MRI examination failure because of claustrophobia (1 patient), or different contrast agent injection rates (3 patients). In total, 28 patients were enrolled. Patients' demographic characteristics, tumor volume and the tumor stage are shown in Table 3. A significant correlation was found between tumor size and stage (P = 0.013, r = 0.463). Neither tumor size nor tumor stage significantly correlated with any of the pharmacokinetic parameters obtained in any of the models.

DCE-MRI microvascular physiopathological parameters obtained with the dual-input two-compartment tracer kinetic model are shown in Table 4. There were no significant differences in the k_{ep}, v_p, or HPI between the dual-input extended Tofts model and the dual-input 2CXM (P = 0.524, P = 0.569, P = 0.622, respectively). Except for v_e, all equivalent pharmacokinetic parameters derived from the two tracer kinetic models are correlated: both F_p and PS in the dual-input 2CXM are correlated with K^{trans} in the dual-input extended Tofts model (P =0.002, r = 0.566; P =0.002, r = 0.570, respectively; Figure 4); k_{ep}, v_p, and HPI were positively correlated (P = 0.001, r = 0.594; P = 0.0001, r = 0.686; P = 0.04, r = 0.391, respectively; Figures 5-7). v_e was significantly less in the dual-input extended Tofts model than in the dual-input 2CXM (P = 0.004), and there was no significant correlation between the two proposed tracer kinetics models (P = 0.156, r = 0.276; Table 4, Figure 8). The value of F_p was larger than that of PS in the dual-input 2CXM (F_P = 1.07 mL/mL per minute, PS = 0.19 mL/mL per minute); K^{trans} derived from the dual-input extended Tofts model was 0.29 min^{-1}; HPI was 0.66 and 0.63 in the dual-input extended Tofts model and the dual-input 2CXM, respectively (Table 4).

DISCUSSION

In recent decades, non-surgical therapies, such as antiangiogenic targeted drugs, radiofrequency ablation, and TACE, play an important role in the HCC therapy regime, and the therapeutic efficacy evaluation of these therapy methods has become an important issue. Response Evaluation Criteria In Solid Tumors

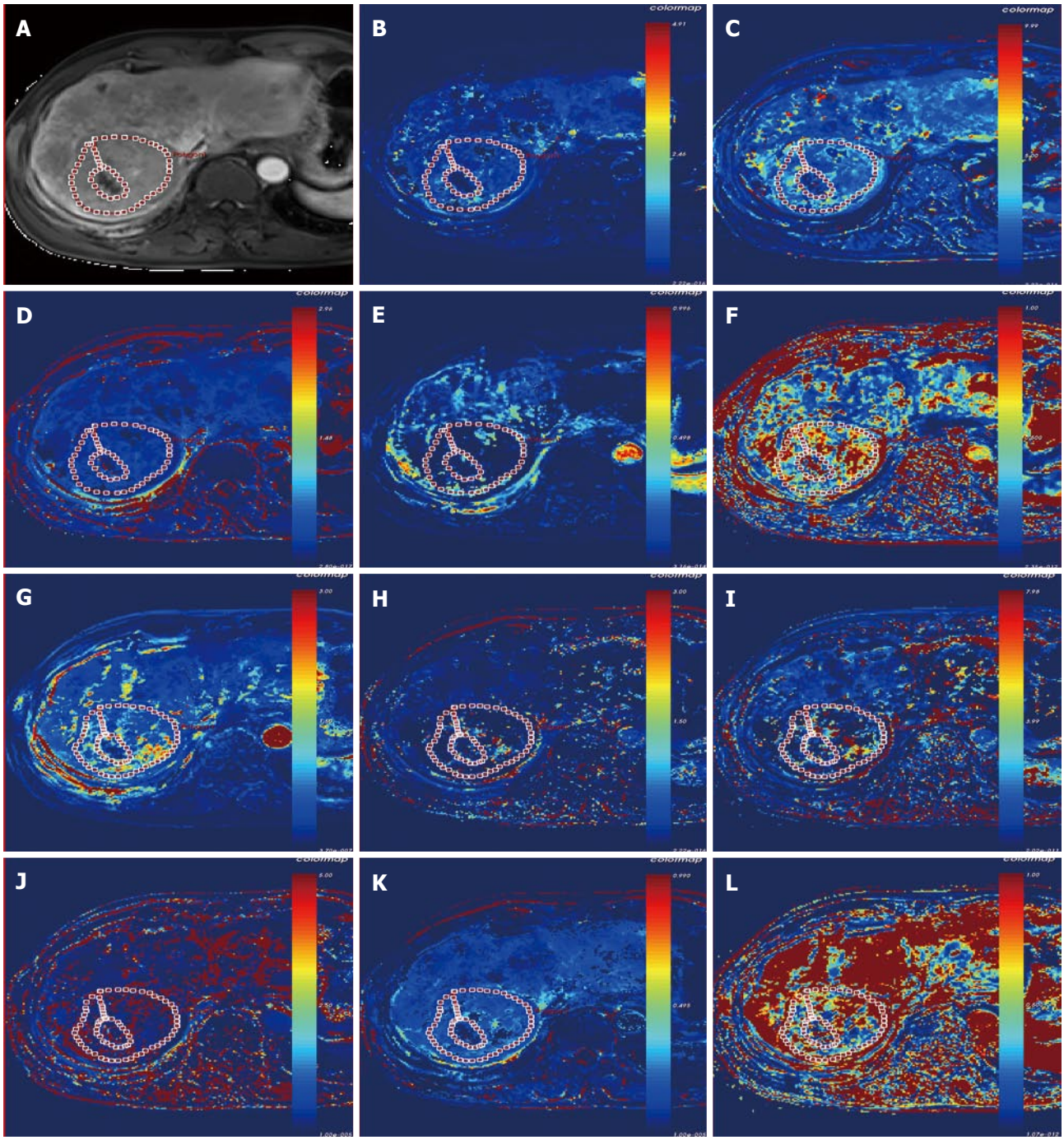

Figure 3 Lesion of the hepatocellular carcinoma in a 68-year-old man on dynamic contrast-enhanced T1WI (A); pharmacokinetic parameter map (K_{trans}, k_{ep}, v_e, v_p, and hepatic perfusion index) derived from the dual-input extended Tofts model (B-F), and the pharmacokinetic parameter maps (F_p, PS, k_{ep}, v_e, v_p, and hepatic perfusion index) derived from the dual-input 2-compartment exchange model (G-L).

(RECIST) or modified RECIST (mRECIST) are common criteria in evaluating a therapeutic effect. Specifically, mRECIST takes into account the contrast enhancement in the arterial phase to evaluate the viable tumor component[16,17]. These modified evaluation criteria imply that the assessment of tumor vascular properties not only contributes to HCC diagnosis but also is helpful in evaluating the therapeutic efficacy of treatments for this tumor. Recently, research has suggested that DCE-MRI allows the quantitative measurement of pharmacokinetic parameters related to perfusion and permeability and provides a more comprehensive assessment of a tumor's physiologic properties[7]. However, finding a suitable tracer kinetic model that takes into account the actual physiopathological status to evaluate the tumor microvascular parameters under the condition of sufficient MRI temporal resolution and spatial resolution is critical.

Several studies have assessed the microvascular properties of HCC using single-input, single-compart-

Table 3 Patients' demographic characteristics, tumor volume, and tumor stage

Age (yr)	Gender	Diagnosis criteria	Size (cm³)	Stage (BCLC)[1]
64.857 ± 10.384	Female 5	Confirmed by histology 8	409.588	A2 (2)
	Male 23	Diagnosed by EASL 20		A3 (3)
				A4 (1)
				B (11)
				C (11)

[1]Barcelona-Clínic Liver Cancer classification[13]. EASL: European Association for the Study of the Liver.

ment or two-compartment tracer kinetic models in monitoring the therapeutic response to interventional therapy or antiangiogenic drug treatment[7,8,18]. However, according to Thng *et al*[11] and Van *et al*[12], the parenchyma in HCC consists of the vascular space and the interstitial space and is supplied by both the portal vein and the hepatic artery in different proportions. We assume that the dual-input two-compartment tracer kinetic model may be suitable for evaluating the microvascular properties of HCC under the conditions of a high field strength MR machine. The purpose of this prospective study was to investigate the feasibility of a dual-input extended Tofts model and a dual-input 2CXM for evaluating microvasculature properties in advanced HCC.

The liver is a hypervascular organ supplied by the portal vein (75%) and the hepatic artery (25%)[19]. However, neovascularization in HCC is predominantly supplied by the hepatic artery, but it is supplemented by the portal vein[20]. HPI describes the relative contribution of arterial *vs* portovenous flow to the total liver perfusion, which is a semi-quantitative descriptor of liver vascularity[11]. In this study, we applied this perfusion parameter to observe the contribution of arterial flow to the HCC in order to verify the assumption that a dual-input model is appropriate in evaluating the pharmacokinetic parameters in most cases of HCC. Our study shows that HPI was 0.66 and 0.63 in the dual-input extended Tofts model and dual-input 2CXM, respectively. This finding is consistent with the assumption that a dual input is a realistic blood supply model in most cases of HCC and also shows that hepatic artery blood flow accounts for the majority but not all of total blood flow to advanced HCC.

K^{trans} is an important pharmacokinetic parameter to assess vascular permeability and therapeutic effects after non-operation treatment in HCC. Previous studies have suggested that a larger drop of K^{trans} is correlated with favorable clinical outcomes after sunitinib or Floxuridine therapy[7,8]. Depending on the balance between PS and F_p in the tissue of interest, K^{trans} has three physiologic interpretations: in a high PS status (PS >> F_p), K^{trans} is approximately equal to F_p; conversely, in high F_p situations (F_p >> PS), K^{trans} is approximately equal to PS; and under mixed flow and permeability limited conditions, K^{trans} is the product (EF_p) of the initial extraction fraction (E) and F_p[21]. Tofts *et al*[21] and Bergamino *et al*[22] noted that the extended Tofts model provides accurate permeability values for only tissues that are weakly vascularized or highly perfused with a relatively high F_p. Our study results show that F_p is greater than PS in the dual-input 2CXM, and the value of K^{trans} in the dual-input extended Tofts model is close to that of PS. Moreover, both F_p and PS are correlated with K^{trans}. These findings are consistent with the second interpretation of the relationship among K^{trans}, F_p, and PS proposed by Tofts *et al*[21] and demonstrate that the dual-input two-compartment tracer kinetic model conforms to the physiologic properties in cases of HCC (high perfusion with relative high F_p) and could be applied to evaluate the perfusion and permeability of pre-therapeutic HCC.

However, the most important role of quantitative DCE-MRI is the assessment of treatment efficacy in advanced HCC after non-surgical methods. These treatments may not produce a change in K^{trans} because F_p and PS may change in opposite directions. On the other hand, F_p and PS may be changed in varying proportions. In these types of situations, it is important to understand which part of the vasculature is affected by the treatment. The dual-input 2CXM is able to provide a separate evaluation of PS and F_p, while the extended Tofts model only provides an assessment of K^{trans}, which reflects a combination of these two parameters; therefore, the dual-input 2CXM may have an advantage over the dual-input extended Tofts model.

k_{ep} is the reflux ratio of the transfer constant between EES and blood plasma. The amounts of k_{ep} in the two models are much larger than the K^{trans} or PS in our study, which also shows no significant difference but certain correlation between the two models with respect to this parameter. As a hypervascular tumor, the contrast agent in the tumor vasculature leaks into EES, and, with the hemodynamics progress, the contrast agent concentration in the EES increases but the tracer in the tumor vasculature decreases because the tracer is not only leaking into EES but also being eliminated from the plasma, which may cause a relative larger k_{ep}. Like K^{trans}, k_{ep} is an important predictable biomarker, and research has shown that a decrease in k_{ep} is correlated with favorable clinical outcomes after antiangiogenic drug treatment[8].

Theoretically, hypervascular tumors are usually composed of a larger vascular space (v_p) relative to the interstitial space (v_e) and show a pattern of rapid arterial enhancement followed by washout, whereas a hypovascular tumor usually consists of a larger v_e relative to the v_p and shows progressive enhancement[10]. However, our study shows that median v_e is far greater than v_p in both the extended Tofts model and the 2CXM model. This result seems

Table 4 Comparison of tumor dynamic contrast-enhanced-magnetic resonance imaging pharmacokinetic parameters from 28 scanned patients using two models [Median (IQR)]

	K^{trans} (min^{-1})	PS (mL/mL · min^{-1})	F_p (mL/mL · min^{-1})	k_{ep} (min^{-1})	v_e	v_p	HPI
Dual-Input Extended Tofts model	0.29 ± 0.38	-	-	1.35 ± 1.42	0.51 ± 1.16	0.12 ± 0.21	0.66 ± 0.24
Dual-Input Exchange model	-	0.19 ± 0.36	1.07 ± 1.73	0.95 ± 1.60	1.22 ± 1.19	0.14 ± 0.17	0.63 ± 0.29
Z/*t* value	NA	NA	NA	-0.638	-2.869	-0.568	0.499[1]
P value	NA	NA	NA	0.524	0.004	0.569	0.622[1]

[1]Paired *t*-test. NA: Not available; HPI: Hepatic perfusion index.

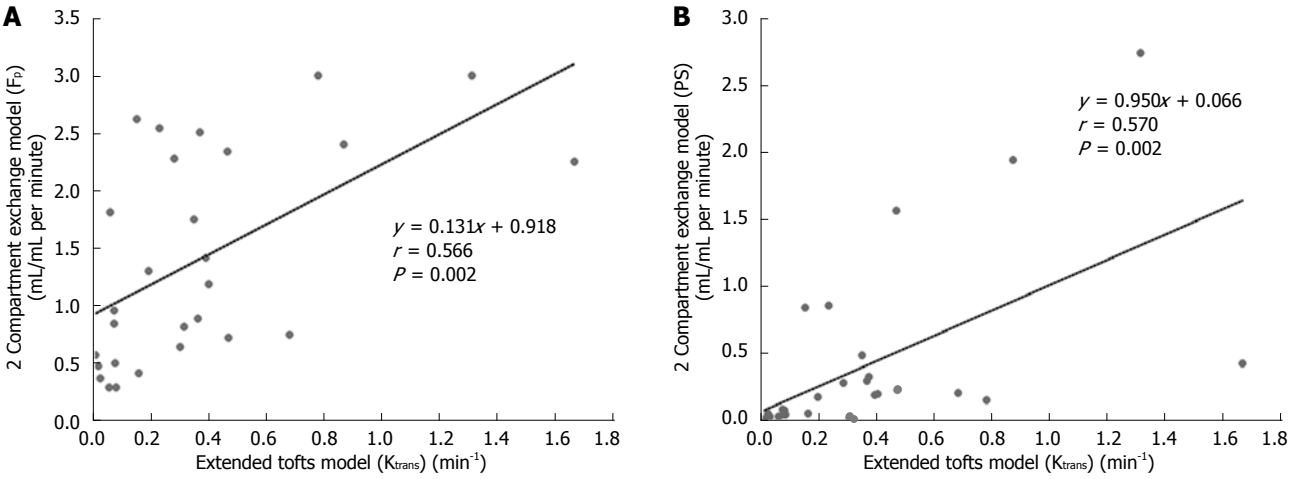

Figure 4 Scatterplots showing the correlation between K^{trans} (min^{-1}) obtained with the extended Tofts model and F_p (A) and PS (B) obtained with the 2-compartment exchange model.

contradictory. The possible reasons for this result are that high blood flow in tumor vasculature results in great hydrodynamic pressure, the contrast agent enters into EES, and the available amount of extracellular space for this tracer to leak into increases; meanwhile, HCC, as a malignant tumor, usually contains a relatively larger EES. An additional reason may be the technology field. One animal DCE-MRI study assessing rat HCC shows that v_e is significantly larger than v_p in the extended Tofts model (also called the extended Kety model). The authors believe that k_{ep} and the sum of v_p and v_e are relatively invariant, and the underestimation of v_p leads to overestimations of v_e which are most severe in the Tofts (Kety) model because v_p is not considered in that model[23]. However, more studies are needed to elucidate the relationship between v_e and v_p.

In this study, v_e is significantly larger in the 2CXM than in the extended Tofts model, with no correlation between the two models. We believed that the relatively lower temporal resolution applied in the 2CXM may have caused this outcome. The 2CXM is more complicated and requires a higher temporal resolution than the extended Tofts model[22]. We acquired data for the 2CXM and the extended Tofts model using the same temporal resolution (6 second), which may have caused the v_e derived from the 2CXM to be overestimated.

There is no significant correlation between tumor size and stage and the microvascular perfusion and permeability in HCC. We believe the main reason for this result is the component we selected to measure the microvascular properties in HCC because we avoid the necrosis, hemorrhage, and adipose degeneration in the tumors, and these pathologic changes are usually relative to the tumor size and stage.

Some limitations of our study should be noted. First, no standard reference was used for any of the parameters. The perfusion and permeability parameters are functional biomarkers, and these parameters could not be measured from the pathological sample *in vitro*. We unavoidably used a well-known consensus as a reference standard that advanced HCC is supplied by the hepatic artery and portal vein with relatively high perfusion. We did not obtain histopathologic confirmation in the 18 HCC patients diagnosed by EASL criteria, as we did not know the grade of the tumor and the degree of cirrhosis around the mass. HCC grade may have influenced the parameters of perfusion and permeability. To date, most research related to HCC has not mentioned the relationship between the grade and the microvascular properties, and we believe it is worthy of future study. Second, the sample size is relatively small, and the relationship between v_e and v_p must be further validated in larger prospective studies.

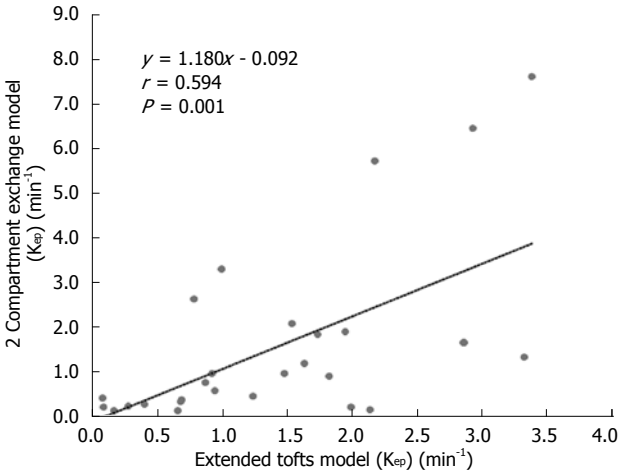

Figure 5 Scatterplot showing the significant correlation of Kep estimated with the extended Tofts model and the 2-compartment exchange model.

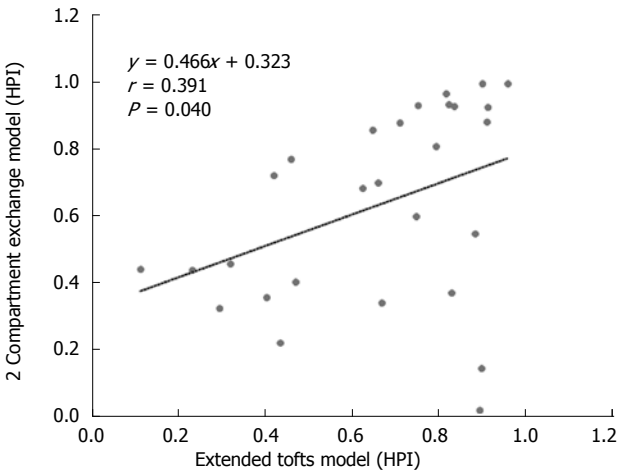

Figure 7 Scatterplot showing the correlation of hepatic perfusion index estimated with the extended Tofts model and the 2-compartment exchange model.

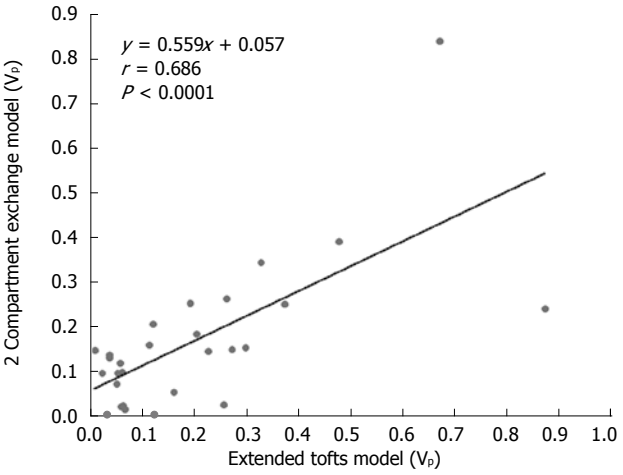

Figure 6 Scatterplot showing that v_p values are correlated between the extended Tofts model and the 2-compartment exchange model.

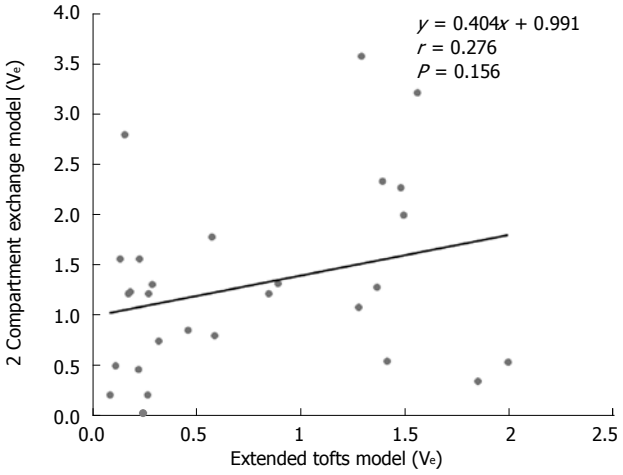

Figure 8 Scatterplot showing that v_e is not correlated in the extended Tofts model and the 2-compartment exchange model.

In addition, the temporal resolution of the acquired image data in this study is 6 s. This resolution may not be high enough for the 2CXM model to measure the tumor interstitial parameter v_e. Finally, patients were instructed to freely breathe during imaging acquisition; this operation method and the patients' heart beat may together result in movement artifacts. We used non-rigid registration as much as possible to diminish the influence of imaging quality caused by movement artifacts.

In conclusion, all of the results derived from this prospective study indicate that the dual-input two-compartment tracer kinetic model could reflect the microvascular properties before the treatment of advanced HCC. Additionally, the dual-input extended Tofts model is more stable in measuring the v_e due to the suitable temporal resolution. Considering the therapeutic efficacy assessment of HCC treated by the antiangiogenic targeted drug, TACE, and radiofrequency ablation, the dual-input 2CXM may be more detailed and accurate than the dual-input extended Tofts model because the dual-input 2CXM can separately evaluate F_p and PS. This function is especially important if F_p and PS may change in opposite directions because K_{trans} cannot reflect this change in the extended Tofts model. However, this assumption needs to be adequately verified by comparing microvasculature parameters derived from the two tracer kinetic models in advanced HCC after antiangiogenic-targeted drug treatment or TACE and is also one of the major purposes of our next study.

ACKNOWLEDGMENTS

The authors thank Dr. Xiao Xu, Dr. Zihua Su and Dr. Ning Wang, GE Healthcare (China), for their assistance in DCE-MRI analysis.

COMMENTS

Background

The parenchyma in hepatocellular carcinoma (HCC) consists of the vascular and interstitial space and is supplied by both the portal vein and the hepatic artery in different proportions; however, to date, the assessment of microvascular properties using a dual-input two-compartment tracer kinetic model with commonly used extracellular gadoliniun contrast agent has not been reported in HCC in a clinical practice setting.

Research frontiers

Some studies have shown the value of assessing microvascular properties in monitoring the effects of interventional therapy or antiangiogenic drug treatment of HCC, as well as metastases in the liver, using single-input single compartment, single-input two-compartment or dual-input single-compartment tracer kinetic models to evaluate a tumor's pharmacokinetic parameters. This study was designed to confirm that a dual-input two-compartment tracer kinetic model could be applied in advanced HCC.

Innovations and breakthroughs

This is the first study to explore and confirm that the dual-input two-compartment tracer kinetic model is suitable to evaluate microvascular physiologic properties in advanced HCC.

Applications

A dual-input two-compartment tracer kinetic model should be applied in assessing tumor microvascular pharmacokinetic parameters in advanced HCC.

Terminology

Dynamic contrast-enhanced-magnetic resonance imaging (MRI) is one of the functional imaging methods of MRI and is used to evaluate microvascular perfusion and permeability in lesions by observing pharmacokinetic parameters.

Peer-review

Although this manuscript is quite "technical", it is interesting to read (also from the clinical point of view). Potential shortcomings (*e.g.*, the rather small sample size) of the study are duly mentioned by the authors at the end of the "discussion".

REFERENCES

1 **Pang TC**, Lam VW. Surgical management of hepatocellular carcinoma. *World J Hepatol* 2015; **7**: 245-252 [PMID: 25729479 DOI: 10.4254/wjh.v7.i2.245]

2 **Corona-Villalobos CP**, Halappa VG, Geschwind JF, Bonekamp S, Reyes D, Cosgrove D, Pawlik TM, Kamel IR. Volumetric assessment of tumour response using functional MR imaging in patients with hepatocellular carcinoma treated with a combination of doxorubicin-eluting beads and sorafenib. *Eur Radiol* 2015; **25**: 380-390 [PMID: 25226843 DOI: 10.1007/s00330-014-3412-6]

3 **O'Connor JP**, Rose CJ, Jackson A, Watson Y, Cheung S, Maders F, Whitcher BJ, Roberts C, Buonaccorsi GA, Thompson G, Clamp AR, Jayson GC, Parker GJ. DCE-MRI biomarkers of tumour heterogeneity predict CRC liver metastasis shrinkage following bevacizumab and FOLFOX-6. *Br J Cancer* 2011; **105**: 139-145 [PMID: 21673686 DOI: 10.1038/bjc.2011.191]

4 **Teo QQ**, Thng CH, Koh TS, Ng QS. Dynamic contrast-enhanced magnetic resonance imaging: applications in oncology. *Clin Oncol (R Coll Radiol)* 2014; **26**: e9-20 [PMID: 24931594 DOI: 10.1016/j.clon.2014.05.014]

5 **Hirashima Y**, Yamada Y, Tateishi U, Kato K, Miyake M, Horita Y, Akiyoshi K, Takashima A, Okita N, Takahari D, Nakajima T, Hamaguchi T, Shimada Y, Shirao K. Pharmacokinetic parameters from 3-Tesla DCE-MRI as surrogate biomarkers of antitumor effects of bevacizumab plus FOLFIRI in colorectal cancer with liver metastasis. *Int J Cancer* 2012; **130**: 2359-2365 [PMID: 21780098 DOI: 10.1002/ijc.26282]

6 **De Bruyne S**, Van Damme N, Smeets P, Ferdinande L, Ceelen W, Mertens J, Van de Wiele C, Troisi R, Libbrecht L, Laurent S, Geboes K, Peeters M. Value of DCE-MRI and FDG-PET/CT in the prediction of response to preoperative chemotherapy with bevacizumab for colorectal liver metastases. *Br J Cancer* 2012; **106**: 1926-1933 [PMID: 22596235 DOI: 10.1038/bjc.2012.184]

7 **Jarnagin WR**, Schwartz LH, Gultekin DH, Gönen M, Haviland D, Shia J, D'Angelica M, Fong Y, Dematteo R, Tse A, Blumgart LH, Kemeny N. Regional chemotherapy for unresectable primary liver cancer: results of a phase II clinical trial and assessment of DCE-MRI as a biomarker of survival. *Ann Oncol* 2009; **20**: 1589-1595 [PMID: 19491285 DOI: 10.1093/annonc/mdp029]

8 **Sahani DV**, Jiang T, Hayano K, Duda DG, Catalano OA, Ancukiewicz M, Jain RK, Zhu AX. Magnetic resonance imaging biomarkers in hepatocellular carcinoma: association with response and circulating biomarkers after sunitinib therapy. *J Hematol Oncol* 2013; **6**: 51 [PMID: 23842041 DOI: 10.1186/1756-8722-6-51]

9 **Khalifa F**, Soliman A, El-Baz A, Abou El-Ghar M, El-Diasty T, Gimel'farb G, Ouseph R, Dwyer AC. Models and methods for analyzing DCE-MRI: a review. *Med Phys* 2014; **41**: 124301 [PMID: 25471985 DOI: 10.1118/1.4898202]

10 **Sourbron SP**, Buckley DL. Tracer kinetic modelling in MRI: estimating perfusion and capillary permeability. *Phys Med Biol* 2012; **57**: R1-33 [PMID: 22173205 DOI: 10.1088/0031-9155/57/2/R1]

11 **Thng CH**, Koh TS, Collins DJ, Koh DM. Perfusion magnetic resonance imaging of the liver. *World J Gastroenterol* 2010; **16**: 1598-1609 [PMID: 20355238]

12 **Van Beers BE**, Daire JL, Garteiser P. New imaging techniques for liver diseases. *J Hepatol* 2015; **62**: 690-700 [PMID: 25457198 DOI: 10.1016/j.jhep.2014.10.014]

13 **European Association For The Study Of The Liver**; European Organisation For Research And Treatment Of Cancer. EASL-EORTC clinical practice guidelines: management of hepatocellular carcinoma. *J Hepatol* 2012; **56**: 908-943 [PMID: 22424438 DOI: 10.1016/j.jhep.2011.12.001]

14 **Donaldson SB**, West CM, Davidson SE, Carrington BM, Hutchison G, Jones AP, Sourbron SP, Buckley DL. A comparison of tracer kinetic models for T1-weighted dynamic contrast-enhanced MRI: application in carcinoma of the cervix. *Magn Reson Med* 2010; **63**: 691-700 [PMID: 20187179 DOI: 10.1002/mrm.22217]

15 **Tofts PS**. Modeling tracer kinetics in dynamic Gd-DTPA MR imaging. *J Magn Reson Imaging* 1997; **7**: 91-101 [PMID: 9039598]

16 **Bruix J**, Sherman M, Llovet JM, Beaugrand M, Lencioni R, Burroughs AK, Christensen E, Pagliaro L, Colombo M, Rodés J. Clinical management of hepatocellular carcinoma. Conclusions of the Barcelona-2000 EASL conference. European Association for the Study of the Liver. *J Hepatol* 2001; **35**: 421-430 [PMID: 11592607]

17 **Llovet JM**, Di Bisceglie AM, Bruix J, Kramer BS, Lencioni R, Zhu AX, Sherman M, Schwartz M, Lotze M, Talwalkar J, Gores GJ. Design and endpoints of clinical trials in hepatocellular carcinoma. *J Natl Cancer Inst* 2008; **100**: 698-711 [PMID: 18477802 DOI: 10.1093/jnci/djn134]

18 **Lee SH**, Hayano K, Zhu AX, Sahani DV, Yoshida H. Dynamic Contrast-Enhanced MRI Kinetic Parameters as Prognostic Biomarkers for Prediction of Survival of Patient with Advanced Hepatocellular Carcinoma: A Pilot Comparative Study. *Acad Radiol* 2015; **22**: 1344-1360 [PMID: 26211553 DOI: 10.1016/j.acra.2015.05.012]

19 **Chiandussi L**, Greco F, Sardi G, Vaccarino A, Ferraris CM, Curti B. Estimation of hepatic arterial and portal venous blood flow by direct catheterization of the vena porta through the umbilical cord in man. Preliminary results. *Acta Hepatosplenol* 1968; **15**: 166-171 [PMID: 4878405]

20 **Hayashi M**, Matsui O, Ueda K, Kawamori Y, Gabata T, Kadoya M. Progression to hypervascular hepatocellular carcinoma: correlation with intranodular blood supply evaluated with CT during intraarterial injection of contrast material. *Radiology* 2002;

225: 143-149 [PMID: 12354998]
21 **Tofts PS**, Brix G, Buckley DL, Evelhoch JL, Henderson E, Knopp MV, Larsson HB, Lee TY, Mayr NA, Parker GJ, Port RE, Taylor J, Weisskoff RM. Estimating kinetic parameters from dynamic contrast-enhanced T(1)-weighted MRI of a diffusable tracer: standardized quantities and symbols. *J Magn Reson Imaging* 1999; **10**: 223-232 [PMID: 10508281]
22 **Bergamino M**, Bonzano L, Levrero F, Mancardi GL, Roccatagliata L. A review of technical aspects of T1-weighted dynamic contrast-enhanced magnetic resonance imaging (DCE-MRI) in human brain tumors. *Phys Med* 2014; **30**: 635-643 [PMID: 24793824 DOI: 10.1016/j.ejmp.2014.04.005]
23 **Michoux N**, Huwart L, Abarca-Quinones J, Dorvillius M, Annet L, Peeters F, Van Beers BE. Transvascular and interstitial transport in rat hepatocellular carcinomas: dynamic contrast-enhanced MRI assessment with low- and high-molecular weight agents. *J Magn Reson Imaging* 2008; **28**: 906-914 [PMID: 18821616 DOI: 10.1002/jmri.21524]

P- Reviewer: Cerwenka HR **S- Editor**: Ma YJ **L- Editor**: Wang TQ
E- Editor: Zhang DN

Published by **Baishideng Publishing Group Inc**
8226 Regency Drive, Pleasanton, CA 94588, USA
Telephone: +1-925-223-8242
Fax: +1-925-223-8243
E-mail: bpgoffice@wjgnet.com
Help Desk: http://www.wjgnet.com/esps/helpdesk.aspx
http://www.wjgnet.com

ISSN 1007-9327